Application of contracted distributed approximating functions to solving vibrational eigenvalue problems

Viktor Szalay and Sean C. Smith

Citation: The Journal of Chemical Physics **110**, 72 (1999); doi: 10.1063/1.478086

View online: http://dx.doi.org/10.1063/1.478086

View Table of Contents: http://scitation.aip.org/content/aip/journal/jcp/110/1?ver=pdfcov

Published by the AIP Publishing

Application of contracted distributed approximating functions to solving vibrational eigenvalue problems

Viktor Szalay[a] and Sean C. Smith
Department of Chemistry, The University of Queensland, Brisbane, Qld 4072, Australia

(Received 10 August 1998; accepted 23 September 1998)

It has been shown that an approximately band-limited function can be reconstructed by using the function's values taken at appropriate equidistant grid points and a generalized Hermite-contracted-continuous-distributed-approximating-function (Hermite-CCDAF) as the reconstruction function. A sampling theorem prescribing the possible choices of grid spacing and DAF parameters has been derived and discussed, and discretized-Hermite-contracted DAFs have been introduced. At certain values of its parameters the generalized Hermite-CCDAF is identical to the Shannon–Gabor-wavelet-DAF (SGWDAF). Simple expressions for constructing the matrix of a vibrational Hamiltonian in the discretized-Hermite-contracted DAF approximation have been given. As a special case the matrix elements corresponding to sinc-DVR (discrete variational representation) are recovered. The usefulness and properties of sinc-DVR and discretized-Hermite-contracted-DAF (or SGWDAF) in bound state calculations have been compared by solving the eigenvalue problem of a number of one- and two-dimensional Hamiltonians. It has been found that if one requires that the same number of energy levels be computed with an error less than or equal to a given value, the SGWDAF method with thresholding is faster than the standard sinc-DVR method. The results obtained with the Barbanis Hamiltonian are described and discussed in detail. © *1999 American Institute of Physics.*
[S0021-9606(99)00501-2]

I. INTRODUCTION

When modeling vibrational spectra of molecules one may be required to calculate both low and high lying states of a vibrational Hamiltonian with a precision (set by the experimental data and/or the theoretical approximations employed) smaller than numerical accuracy attainable by the computer. In a variational or a discrete variable representation (DVR) calculation, however, the accuracy of the calculated energy levels gradually decreases from high accuracy to low as one progresses from low to high lying states. Thus, it might be suggested that one wastes computational effort on calculating the lower states with an accuracy which may not be needed. In this paper we present a method suitable for calculating lower and higher states with similar accuracy simultaneously. Since no numerical effort is wasted the computations are faster as is demonstrated by simple numerical examples. Our method is based on employing a discretized form of contracted-continuous-distributed-approximating-functions (CCDAFs)[1] in setting up the matrix representation of the vibrational Schrödinger equation. It has been found that the matrix elements required can be given by simple analytical expressions whose limiting case is the well known sinc DVR.[2]

The outline of the paper is as follows. Section II gives a brief definition of CCDAFs. A sampling theorem designed for approximating the Hermite-CCDAF integral by a quadrature of equidistant points is developed and discretized-Hermite-contracted-DAFs are introduced in Sec. III. Then, the matrix elements of the potential and kinetic energy operators of simple vibrational Hamiltonians are derived employing the discretized-Hermite-contracted-DAF approximation (Sec. IV). Results of numerical applications to one- and two-dimensional Hamiltonians are presented, discussed, and compared to those for the sinc-DVR in Sec. V. Section VI summarizes the paper.

II. CONTRACTED-CONTINUOUS-DISTRIBUTED-APPROXIMATING FUNCTIONS

CCDAFs provide an approximation of a function, say $\Psi(x)$, by the integral

$$\Psi(x) \simeq \Psi_{\mathrm{app}}(x) = \int dz\ K(z;s)\Psi(z+x), \tag{1}$$

where the function $K(z;s)$ of parameters s, derived from standard orthogonal polynomials through a contraction procedure,[1] is called a CCDAF. The CCDAFs approach the Dirac distribution $\delta(z)$ by taking the appropriate limit of their parameters.

One of the simplest CCDAFs is derived with Hermite functions and is given in a slightly generalized form by the equation

$$K(z;\alpha,M) = e^{-\alpha^2 z^2}\frac{1}{\pi}\frac{\sin Mz}{z} \quad (z\in[-\infty,\infty]). \tag{2}$$

Figure 1 depicts the Hermite-CCDAF along with its momentum space form (related by a Fourier transform in this case) at different values of its parameters. By taking the Fourier

[a]Permanent address: Crystal Physics Department, Institute for Solid State Physics and Optics, Hungarian Academy of Sciences, P.O. Box 49, H-1523 Budapest, Hungary; electronic mail: szalay@chemistry.uq.edu.au

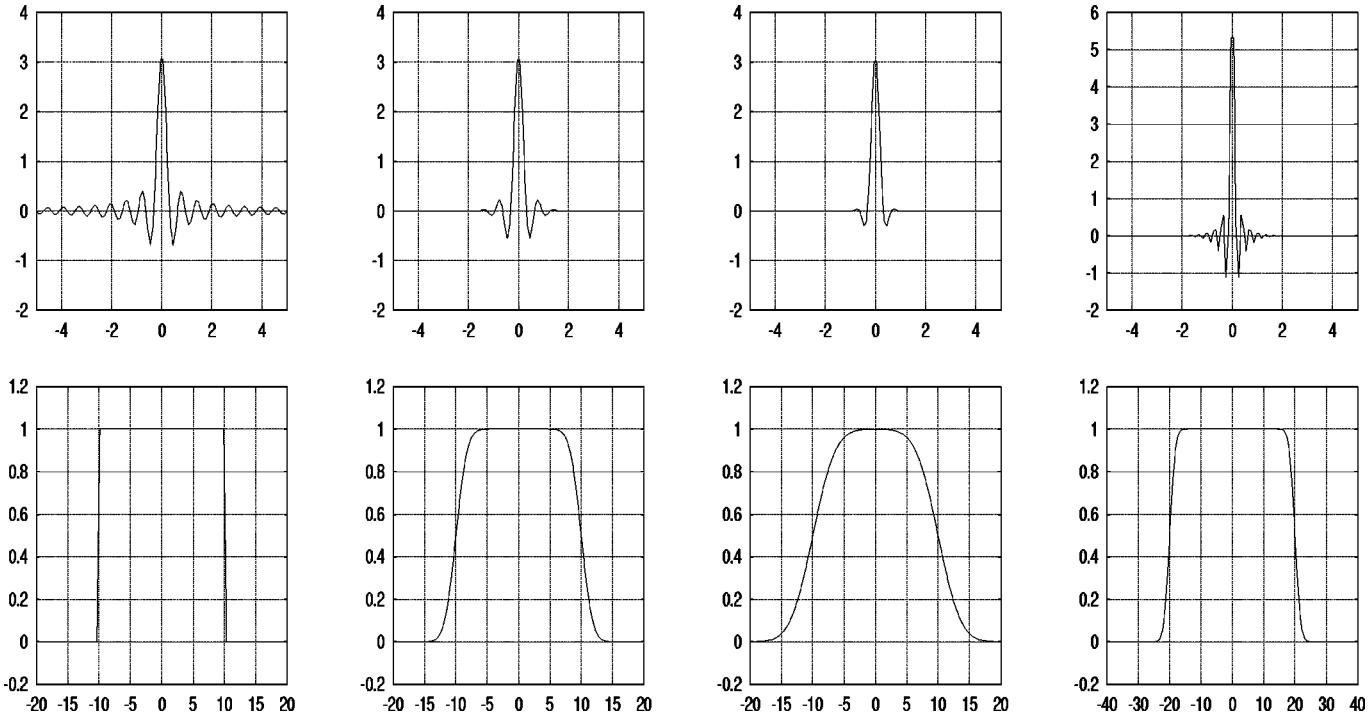

FIG. 1. The pictures in the first row depict, from left to right, generalized Hermite-CCDAFs of parameters ($\alpha=0.01$, $M=10$), ($\alpha=1$, $M=10$), ($\alpha=2$, $M=10$), and ($\alpha=1$, $M=20$), respectively. The corresponding momentum space DAFs are shown in the second row.

transform of both sides in Eq. (1) one can see that any function $\Psi(x)$ whose transform falls within the range of the CCDAF plateau can be well approximated by the CCDAF integral [i.e., Eq. (1)]. The parameter M controls the width of the plateau while α controls the rate of decay of the plateau.

III. DISCRETIZED CONTRACTED-HERMITE-CCDAFS

CCDAFs may be used to obtain a matrix representation of the Schrödinger equation by changing variable ($z+x \rightarrow y$) and approximating the integral in the CCDAF approximation by suitable quadrature. It would be the simplest to employ an equidistant grid. The question, then is how the grid spacing should be chosen to achieve reasonable accuracy. We shall answer this question for the case of the Hermite-CCDAF. Since Hermite-CCDAFs are approximately band limited we can employ the ''δ'' method[3] and derive a sampling theorem. The procedure may not be well known, therefore we shall describe it in detail.

A sampled form of $\Psi(x)$ may be written as

$$\Psi_s(x)=\Psi(x)\sum_n \delta(x-n\tau)=\sum_n \Psi(n\tau)\delta(x-n\tau)$$

$$\tau>0;n=0,\pm 1,\pm 2,\ldots, \quad (3)$$

where τ denotes the grid spacing. In analogy to Eq. (3), we aim at reconstructing $\Psi(x)$ from its sampled values with the help of a Hermite-CCDAF as the reconstruction function, that is we have:

$$\Psi(x)=\Psi_{\text{app}}(x)=\sum_n \Psi(n\tau)K(x-n\tau) \quad (4)$$

$$=\int_{\infty}^{\infty} du\ \Psi(u)K(x-u)\sum_n \delta(u-n\tau). \quad (5)$$

By substituting the Fourier expansion of the impulse train,

$$\sum_n \delta(u-n\tau)=\frac{1}{\tau}\sum_n \exp\left(-\frac{2\pi i n u}{\tau}\right), \quad (6)$$

into Eq. (5) and taking the Fourier transform of both sides one obtains the relation,

$$\hat{\Psi}(k)=\frac{1}{\tau}\sqrt{2\pi}\hat{K}(k)\sum_n \hat{\Psi}\left(k+\frac{2\pi n}{\tau}\right). \quad (7)$$

Now, assume that Ψ is band limited to $(-\pi W,\pi W)$ and examine Eq. (7). The sum on the right side is a sum of shifted copies of $\hat{\Psi}$. The copies will overlap if the length of shift is smaller than the bandwidth, i.e.,

$$\frac{2\pi}{\tau}<2\pi W, \quad (8)$$

while there is no overlap if

$$\frac{2\pi}{\tau}>2\pi W. \quad (9)$$

Since there is just a single copy of $\hat{\Psi}$ on the left side of Eq. (7), the function

$$\frac{1}{\tau}\sqrt{2\pi}\hat{K}(k)$$

must be such that it can filter just a single copy of $\hat{\Psi}$. As seen from Fig. 1 the Hermite-CCDAF may serve as a filter function.

Overlapping $\hat{\Psi}$s can lead to aliasing unless the filter is adjusted properly. Even then, only part of Ψ can be recovered. To avoid aliasing and achieve a complete reconstruction the grid spacing should be chosen such that

$$\tau \leqslant \frac{1}{W}. \tag{10}$$

Equation (10) together with the band-limited property of Ψ is called the Niquist sampling theorem.[4,5] Since the functions to be reconstructed are, in general, only approximately band limited we choose a grid spacing satisfying the stricter condition

$$\tau \leqslant \frac{1}{rW}, \tag{11}$$

where $r>1$.

Having derived the sampling theorem we can now write the discretized version of the Hermite-CCDAF approximation as

$$\Psi(x) \simeq \Psi_{\text{app}}(x) = \sum_n \Psi(n\tau) e^{-\alpha^2 (x-n\tau)^2} \times \frac{\sin M(x-n\tau)}{\pi(x-n\tau)} \tau. \tag{12}$$

The set of functions

$$\left\{ e^{-\alpha^2 (x-n\tau)^2} \frac{\sin M(x-n\tau)}{\pi(x-n\tau)} \tau \right\}_n$$

will be called discretized-Hermite-contracted-DAF.

Given the bandwidth of the function Ψ and an appropriately chosen τ, one still has to put some constraint on the bandwidth of the reconstruction function to avoid filtering more than one copy of $\hat{\Psi}$ or just part of $\hat{\Psi}$. The choice

$$M = r\pi W \tag{13}$$

is, in general, appropriate.

Since πW is related to energy as

$$\pi W = \frac{f}{\hbar} \sqrt{2 m_{\text{eff}} E}, \tag{14}$$

the number of grid points, $\mathcal{N}$, required to satisfactorily approximate eigenstates of energy $E_{\max}$ or lower than $E_{\max}$ obeys the inequality

$$\mathcal{N} = \frac{x_{\max} - x_{\min}}{\tau} \geqslant (x_{\max} - x_{\min}) r \frac{1}{\pi} \frac{f}{\hbar} \sqrt{2 m_{\text{eff}} E_{\max}}, \tag{15}$$

where f is a scaling parameter of dimension of length, $x_{\max}$ and $x_{\min}$ stand for the classical turning points of a particle of effective mass m_{eff} and energy $E_{\max}$ moving in the potential surface $V(x)$, x is a dimensionless variable, and the zero of energy scale is chosen so that all sates have energy equal to or larger than zero. Equation (15) states that the number of grid points must be larger than or equal to the product of the volume explored by the classical (i.e., not quantum) particle and the number of de Broglie wavelengths in unit volume.

IV. MATRIX REPRESENTATION OF THE SCHRÖDINGER EQUATION BY DISCRETIZED HERMITE-CONTRACTED-DAFS

In this work, we consider Hamiltonians of the form

$$\hat{H} = -\sum_{i=1}^{N} \frac{\hbar^2}{2m_i} \frac{\partial^2}{\partial x_i^2} + V(x_1, x_2, \ldots, x_N). \tag{16}$$

We present formulas just for the case $N=1$. However, it will be apparent that one can obtain the formulas valid for larger Ns by taking the appropriate direct products. In deriving the matrix elements we employ the collocation principle, that is we let the Hamiltonian act on Ψ_{app} and calculate the value of the resulting function at the grid points $n\tau$, $n=0,\pm 1, \pm 2, \ldots, \pm(\mathcal{N}-1)/2$,

$$(\hat{H}\Psi_{\text{app}})|_{n\tau} = \epsilon \Psi_{\text{app}}|_{n\tau}, \tag{17}$$

where Ψ_{app} is the discretized-Hermite-contracted-DAF approximation to Ψ. The grid spacing, τ, is assumed to be the optimal one defined by equality in Eq. (11) and M is chosen according to Eq. (13) (thus $M\tau = \pi$).

A. Matrix elements of the potential energy operator

The matrix elements of the potential energy operator are given as

$$V_{mn} = V(m\tau)\delta_{mn}, \tag{18}$$

since

$$\begin{aligned} V(x)\Psi_{\text{app}}(x)|_{m\tau} &= V(m\tau)\Psi_{\text{app}}(m\tau) \\ &\simeq V(m\tau) \sum_n \Psi(n\tau) e^{-\alpha^2 (m-n)^2 \tau^2} \\ &\quad \times \frac{\sin \pi(m-n)}{\pi(m-n)} \\ &= \Psi(m\tau) V(m\tau) \delta_{mn}, \end{aligned} \tag{19}$$

where we have made use of the relations $M\tau = \pi$ and

$$\frac{\sin \pi(m-n)}{\pi(m-n)} = \delta_{mn}. \tag{20}$$

B. Matrix elements of d^2/dx^2

The derivation is straightforward and outlined in the appendix. We obtained the following simple analytical expressions:

$$\left(\frac{d^2}{dx^2}\right)_{mn} = e^{-\alpha^2 j^2 \tau^2} \left(\frac{1}{\tau^2} \frac{2}{j^2} + 4\alpha^2 \right) (-1)^{j+1}$$

$$j = m-n, \quad m \neq n, \tag{21}$$

$$\left(\frac{d^2}{dx^2}\right)_{mm} = -\left(2\alpha^2 + \frac{\pi^2}{3\tau^2} \right). \tag{22}$$

In the special, $\alpha=0$ case these formulas simplify to that of the sinc-DVR by Colbert and Miller.[2]

V. APPLICATIONS AND DISCUSSION

One can show that the approximation in Eq. (12) with the optimal grid spacing and the particular choice of M given by Eq. (13) is identical to the one obtained by the Shannon-Gabor-wavelet-DAF (SGWDAF).[6,7] This is interesting for we arrived at the same result from an approach significantly different from that in Refs. 6 and 7. Hence, SGWDAFs may be described as generalized Hermite-CCDAFs and vice versa.

Kouri *et al.*[6,7] have already given ample evidence that the approximation in Eq. (12) with Eq. (13) and $\alpha \neq 0$ as applied to function reconstruction can be significantly more accurate than the sinc function approximation ($\alpha=0$). They have also given examples of its application in scattering[7] as well as in bound state[6] calculations. It is the latter problem that we shall study further. Indeed, the analysis of the sampling theorem in Sec. III and the analytic expressions of matrix elements derived in Sec. IV suggest that one should examine whether there are any advantages in using SGWDAFs rather than the simple sinc-DVR in bound state calculations.

We have carried out calculations with several one-dimensional (1D) and 2D Hamiltonians including the harmonic oscillator Hamiltonian, a Hamiltonian with double well potential,[8] a 2D coupled harmonic oscillator Hamiltonian,[8] the Hénon–Heiles Hamiltonian,[9] and the Barbanis Hamiltonian.[10,11] For brevity, we shall not present all of the test results, however, all cases studied have given support to the following general conclusions:

(1) The SGWDAF does not give more accurate eigenvalues nor does it give more eigenvalues with reasonable accuracy, than the sinc-DVR employing the same grid.

(2) However, there is a wide range of α values when the SGWDAF gives results of similar accuracy to those by the sinc-DVR.

(3) The magnitude of the off-diagonal elements of the SGWDAF Hamiltonian matrix decreases fast with increasing α and with increasing distance from the diagonal. The SGWDAF Hamiltonian matrix can be highly banded while still providing results of similar accuracy to that of the non-banded sinc-DVR Hamiltonian matrix.

(4) The bandedness of the SGWDAF Hamiltonian matrix allows one to set to zero all matrix elements of magnitude smaller than a given threshold and carry out matrix vector multiplications in fewer flops (thus in less CPU time) than $O(\mathcal{N}^2)$. In fact, since both the SGWDAF and the sinc-DVR result in a Toeplitz kinetic energy matrix and a diagonal potential matrix, the multiplication of the Hamiltonian matrix and a vector can be done in just $O(\mathcal{N}\log_2\mathcal{N})$ flops. With thresholding, as suggested by Marchioro *et al.*,[12] operation counts as low as $O(\mathcal{N}w)$ or $O(\mathcal{N}\ \log_2\ w)$ (where w is called the bandwidth in Ref. 12; later we shall call $2w+1$ the bandwidth) can be achieved with the SGWDAF Hamiltonian matrix. Thus, by thresholding the SGWDAF matrix the calculations can be made faster than a sinc-DVR calculation. [The operation count $O(\mathcal{N}\log_2\mathcal{N})$ of multiplying a Toeplitz matrix with a vector results from considering that a Toeplitz matrix can be extended to a circulant matrix and the circulant matrix is diagonalized by the Fourier matrix. Thus the matrix–vector multiplication can be recast in terms of calculating discrete Fourier transforms. A recent work on this subject is, for instance, Ref. 13.]

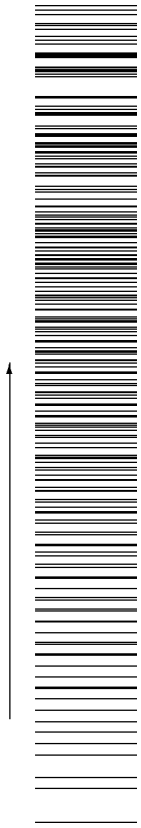

FIG. 2. The distribution of the energy levels of the Barbanis Hamiltonian selected for comparison of sinc-DVR and SGWDAF calculations.

(5) Although thresholding necessarily leads to loss of accuracy, a large number of eigenvalues can be obtained fairly accurately. Interestingly, the number of eigenvalues of acceptable accuracy is almost the same as in the corresponding sinc-DVR calculation, and the low and high lying states can be obtained with approximately the same accuracy. In other words, extreme accuracy of low-energy states is limited, but reasonable accuracy is retained across the spectrum.

As an illustration of the conclusions above we shall present our results for the Barbanis Hamiltonian

$$\hat{H}=-\frac{1}{2}\left(\frac{\partial^2}{\partial x^2}+\frac{\partial^2}{\partial y^2}\right)+\frac{1}{2}(\omega_x^2x^2+\omega_y^2y^2)+\beta xy^2$$

$$\omega_x^2=1.6,\omega_y^2=0.9,\beta=-0.08 \tag{23}$$

studied in Refs. 11 and 14.

Of the rich spectrum we have calculated with the Barbanis Hamiltonian, 203 eigenvalues were selected. All of these are below the dissociation barrier of height 25.313.[11] The highest level (24.010) is about 24 times bigger then the lowest level of value 1.1058. Thus we have an example of an extended and dense spectrum. Figure 2 depicts the distribution of the selected energy levels. The convergence of these levels has been checked with respect to basis size and grid spacing. The chosen levels have been found to be converged with at least ten significant figures. We shall refer to these

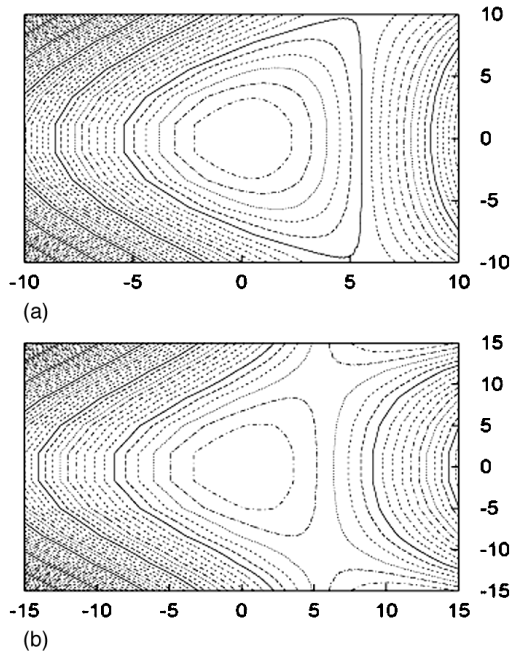

FIG. 3. Contour plot of the region of the Barbanis potential surface explored by our 201-function (a) and 301-function (b) per coordinate basis sets.

levels as the exact ones. They have been assigned in all of our calculations with smaller basis size and/or with thresholding, thus allowing us to make comparisons.

We employed 301 (and 201) SGWDAFs for each coordinate, placed symmetrically around zero with grid spacing 0.1. Thus, the region of configuration space covered is $|x|<15$, $|y|<15$ (and $|x|<10$, $|y|<10$) (see Fig. 3). In Ref. 11 there were 20 harmonic oscillator states employed for each coordinate, where the highest energy basis state involved the 40th Hermite polynomial for the y coordinate and the 19th for the x coordinate. The configuration space explored by this basis set can be estimated by calculating the corresponding Gauss–Hermite DVR. One can find the that $|x|<5.5$ and $|y|<8.3$ (see Fig. 4). Since our basis set has elements outside the dissociation barrier, tunneling effects, although very small, might give rise to levels which are not strictly bound. Such eigenvalues would have little physical meaning, since we have made no attempt to satisfy the required boundary conditions. Regardless, these eigenvalues are still numerically well converged and can be used for our present goal of comparing sinc-DVR and SGWDAF.

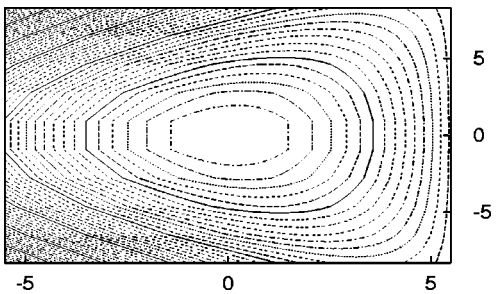

FIG. 4. Contour plot of the region of the Barbanis potential surface explored by the basis set used in Ref. 11.

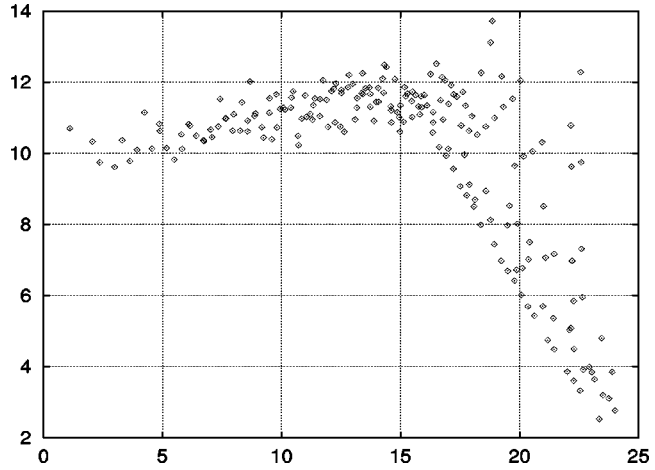

FIG. 5. The relative error (vertical axis) as measured by the quantity defined by Eq. (24) of the energy levels (horizontal axis) calculated with the 201 function per coordinate sinc-DVR.

Although not all of them are selected, we have obtained all the energy levels tabulated in Ref. 11. The highest levels in Ref. 11 appear to be less converged than indicated. (Note that only levels even with respect to reflection about the x axis have been given in Ref. 11.)

Figures 5–8 and the data in Tables I and II illustrate conclusions (1)–(5).

In each figure the eigenvalues, ϵ_i, are drawn along the horizontal axis while the vertical axis displays the quantity

$$s_i = -\log_{10}\left(\frac{\epsilon_i^{\text{exact}} - \epsilon_i}{\epsilon_i^{\text{exact}}}\right) - 2 \tag{24}$$

measuring the relative error of calculated eigenvalues with respect to the exact ones. The data in Figs. 5–8 correspond to calculations with grid spacing 0.1 for each coordinate, with grid points distributed symmetrically around zero, and with α values of 0,0.5,1, and 2, respectively. But in the calculation of the selected ''exact'' eigenvalues, where we used 301

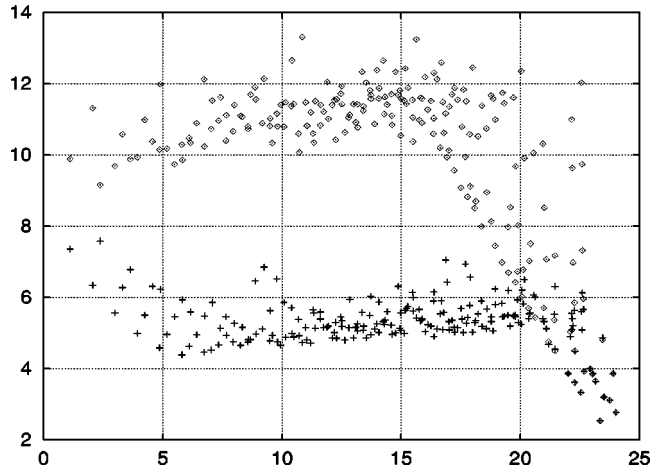

FIG. 6. The relative error of energy levels calculated by the 201 function per coordinate SGWDAF of $\alpha=0.5$ basis: ($\diamond$) relative errors of levels obtained without thresholding, (+) relative error of levels obtained by setting zero all matrix elements of absolute value smaller than 10^{-5} in the SGWDAF Hamiltonian matrix.

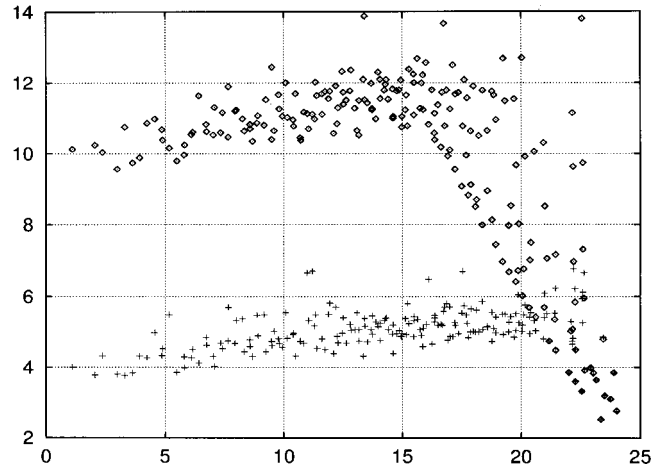

FIG. 7. The same as in Fig. 6, but employing an SGWDAF of $\alpha=1$ basis.

points per coordinate, 201 points per coordinate were used. The Hamiltonian matrices as obtained by the prescriptions in Sec. IV are symmetric and labeled by indices referring to grid points. (Note that the representation constructed similarly for a Hamiltonian with coordinate dependent effective mass would not be symmetric.) The related matrix eigenvalue equations have been solved by using the Lanczos algorithm. We have carried out as many iterations as required to converge the selected eigenvalues such that they have a dispersion (or error norm)[15] smaller than 10^{-11}. 24 000 iterations have been found to be sufficient. Points denoted by ($\diamond$) in Figs. 5–8 correspond to calculations without thresholding. Points denoted by ($+$) in Figs. 5–8 correspond to calculations with thresholding with a threshold value 10^{-5}. At this threshold value and the grid size mentioned the bandwidth of the kinetic energy matrix of each coordinate is 401 for $\alpha=0$, 131 for $\alpha=0.5$, 69 for $\alpha=1$ and 37 for $\alpha=2$. Matrix–vector multiplication routines of scaling $O(\mathcal{N}\log_2\mathcal{N})$ and $O(\mathcal{N}w)$ were employed in the calculations with SGWDAFs of $\alpha=0$ and $\alpha\neq 0$, respectively. The CPU time (in seconds) for performing 24 000 Lanczos iterations was 3305 for $\alpha=0$, 3015 for $\alpha=0.5$, 1870 for $\alpha=1$, and 1197 for $\alpha=2$.

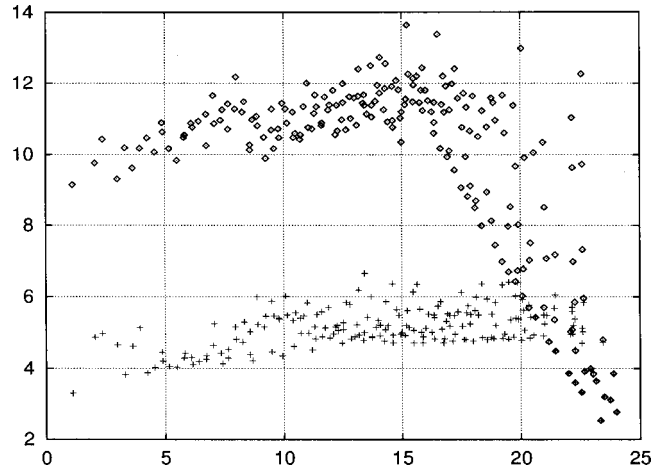

FIG. 8. The same as in Fig. 6, but employing an SGWDAF of $\alpha=2$ basis.

TABLE I. CPU time (in s) consumed by 1500 Lanczos iterations when different matrix–vector multiplication routines are employed in solving the 1D harmonic oscillator's eigenvalue problem. The different routines are distinguished by their scaling properties.

$\mathcal{N}$	$O(\mathcal{N}^2)$	$O(\mathcal{N}\log_2\mathcal{N})$	$O(\mathcal{N}w)$ ($w=18$)	$O(\mathcal{N}\log_2 w)$ ($w=18$)
51	0.07	0.08	0.03	0.12
101	0.27	0.15	0.06	0.23
201	1.08	0.35	0.13	0.55
301	2.38	0.90	0.19	0.85
701	292.41	2.32	0.43	2.19
1501	1560.96	6.47	0.92	4.62

In Tables I and II we have given the CPU times required by programs having different matrix–vector multiplication routines to perform the same number (1500) of Lanczos iterations with matrices of the same size. The different routines are designated by the approximate number of flops they need to carry out one matrix vector multiplication. We have given the timing data only of those codes which were optimized at compile time with the f77 FORTRAN compiler options -O3 -qstrict. The data in Tables I and II refer to calculations on the 1D and 2D harmonic oscillator, respectively. It should be noted that the calculations with matrices of bandwidth $2w+1=37$ ($\alpha=1$) were not only faster but also quite accurate and figures similar to Figs. 5–8 could be drawn. All the calculations were carried out on an IBM RISC6000 workstation.

Comparison of Figs. 5–8 along with the data in Table I and II clearly justify our conclusions. Conclusions (1) and (2) can also be deduced from the fact that by increasing α one slowly destroys the DAF plateau (see Fig. 1) and makes the DAF approximation less accurate.

It is worth noting that the standard matrix vector multiplication routine requiring $O(\mathcal{N}^2)$ flops becomes very slow for matrices of rank greater than 300. In a higher dimensional problem, if one cannot construct a basis set of size smaller than 300 for each degree of freedom, the calculations can become very slow if not impossible. In this case one should employ the sinc-DVR or SGWDAF, since then the matrix vector multiplication can be done efficiently even with matrices of size larger than 300×300. We have found that the matrix–vector multiplication routine which theoretically appears to be the most efficient among those considered [i.e., $O(\mathcal{N}\log_2 w)$ flops] is surprisingly slow. This might be

TABLE II. CPU time (in s) consumed by 1500 Lanczos iterations when different matrix–vector multiplication routines are employed in solving the eigenvalue problem of the 2D harmonic oscillator. $\mathcal{N}$ is the number of basis functions per coordinate. The different routines are distinguished by their scaling properties.

$\mathcal{N}$	$O(\mathcal{N}^2)$	$O(\mathcal{N}\log_2\mathcal{N})$	$O(\mathcal{N}\omega)$ ($w=18$)	$O(\mathcal{N}\log_2 w)$ ($w=18$)
51	6.03	6.96	3.68	13.60
101	64.58	38.01	17.92	63.64
201	477.02	206.19	75.92	290.79
301	1749.27	717.05	256.24	672.44
351	20 494.92	865.26	350.70	902.05

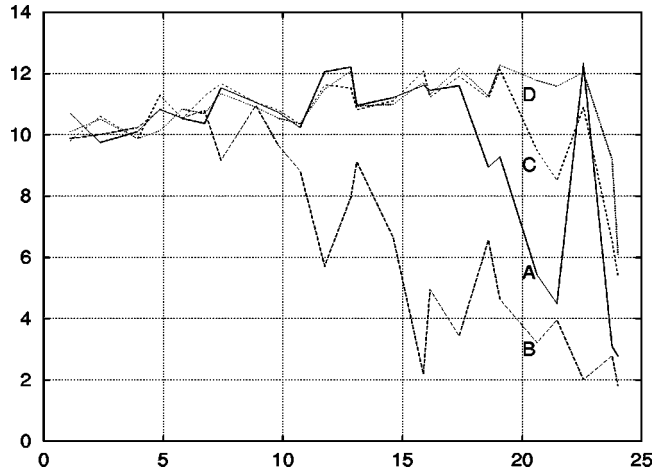

FIG. 9. Comparison of the SGWDAF and Gauss–Hermite DVR results obtained with the Barbanis Hamiltonian. The vertical axis shows the relative error as calculated by Eq. (24). The horizontal axis is the energy axis. Comparisons are made with respect to 24 ''exact'' eigenvalues. The points in the figure are joined by lines just to guide the eye. N_x and N_y denote the number of grid points used for coordinate x and y, respectively. (Curve **A**): The relative error of energy levels obtained by SGWDAF calculation with $\alpha=0$, $N_x=N_y=201$, and 24 000 Lanczos iterations. The calculation required 3305 CPU seconds. (Curve **B**): The relative error of energy levels obtained by Gauss–Hermite DVR calculation with $N_x=21$, $N_y=41$, and 10 000 Lanzcos iterations. The calculation required 29 CPU seconds. (Curve **C**): The relative error of energy levels obtained by Gauss–Hermite DVR calculation with $N_x=41$, $N_y=61$, and 10 000 Lanzcos iterations. The calculation required 40 CPU seconds. (Curve **D**): The relative error of energy levels obtained by Gauss–Hermite DVR calculation with $N_x=N_y=101$, and 20 000 Lanczos iterations. The calculation required 851 CPU seconds.

because our code is simply not efficient enough or maybe because the matrices considered were too small to get to the limit where the scaling $O(\mathcal{N}\log_2 w)$ actually becomes effective.

The choice of basis set is crucial when solving the multidimensional vibrational Schrödinger equation. One should attempt to choose the basis set such that the Hamiltonian matrix in this basis set is both diagonally dominant and structured as much as possible to ensure fast convergence and computation. Which basis set should be used is often suggested by the nature (e.g., the shape of the potential surface) of the problem studied but often it is hard to find a single basis set working equally well in all energy ranges of interest.

We must point out that the problems we used to compare sinc-DVR and SGWDAFs can be solved more efficiently by employing a more natural basis such as the Gauss–Hermite DVR. In fact, the eigenvalues of the Barbanis Hamiltonian can be obtained with high precision with a small Gauss–Hermite DVR basis (see Fig. 9) in a few tens of CPU seconds compared to the few thousand seconds consumed by either the sinc-DVR or SGWDAF calculations.

However, there may not be an obvious choice of a ''good'' basis set when one would like to calculate high lying vibrational states and/or resonances on a complicated strongly anharmonic potential surface. Then, one has to attempt to construct a good basis set by starting from an initial so called primitive basis set, e.g., by employing the method of filter diagonalization.[16] As to the primitive basis set one requires it to provide a simple, structured matrix representation of the Hamiltonian operator such that the calculation of the Hamiltonian matrix as well as the following computational work, whose most crucial operation is the matrix–vector multiplication, can be carried out as fast as possible. The SGWDAFs along with the thresholding procedure give a simple, structured Hamiltonian matrix and there exist fast methods to carry out the Hamiltonian matrix–vector multiplication. Therefore SGWDAFs may be used as a primitive basis to construct an optimal basis set efficiently for any desired energy range.

VI. SUMMARY

It has been shown that an approximately band-limited function can be reconstructed by using the function's values taken at appropriate equidistant grid points and a generalized Hermite-CCDAF as the reconstruction function. What the appropriate grid spacing is and what values may be given to the DAF parameters is determined by the bandwidth of the function to be reconstructed. A sampling theorem prescribing the possible choices of grid spacing and DAF parameters has been derived and discussed. At certain values of the DAF parameters the generalized Hermite-CCDAF is identical to the recently introduced Shannon–Gabor-wavelet-DAF.[6,7]

Since contracted Hermite-DAFs are closely related to the sinc function approximation we have studied how they may be used in solving bound state eigenvalue problems and if there is any advantage of employing them compared to sinc-DVR. While doing so we have derived simple analytical expressions for the matrix elements required to construct the Hamiltonian matrix in the SGWDAF (or in other words in the discretized-Hermite-contracted-DAF) approximation. The matrix elements corresponding to the sinc-DVR[2] are recovered as a special case of our more general formulas.

Based on numerical investigations of a number of 1D and 2D Hamiltonian eigenvalue problems, we have found that the SGWDAF (or contracted Hermite-DAF) gives no more accurate eigenvalues than the corresponding sinc-DVR nor does it give more eigenvalues of reasonable accuracy. It can, however, lead to a highly banded Hamiltonian matrix. At the cost of losing extreme accuracy in the lower part of the spectrum one can set all matrix elements of magnitude smaller than a prescribed threshold equal to zero. Then, making use of the special structure of the Hamiltonian matrix, the matrix–vector multiplication operation required by iterative diagonalization methods can be done very efficiently. Interestingly, both low and high lying states can be obtained with approximately the same precision. To illustrate and justify our conclusions we have presented and discussed our numerical results obtained with the Barbanis Hamiltonian[11] in detail. The calculations with the Barbanis Hamiltonian provide a strict test of our method and conclusions because of the dense and extended nature of its spectrum.

It is apparent that for large scale computations involving multidimensional Hamiltonians SGWDAF or sinc-DVR may be very useful, especially when the basis size for a given coordinate cannot be decreased to at least 300 either by basis set contraction, grid optimization, or by constructing an efficient nondirect product grid. The properties of SGWDAFs

suggest that they can be combined efficiently with the filter diagonalization method[16] to construct a basis set suitable to any desired energy range of the system studied.

ACKNOWLEDGMENTS

We gratefully acknowledge financial support from the Australian Research Council Large Grant Scheme (Grant No. A29701390). One of the authors (VS) has received additional support through Grant No. OTKA T 025103.

APPENDIX

To obtain the matrix elements of the differential operator d^2/dx^2 we evaluate $d^2\Psi_{\rm app}(x)/dx^2$ at $x=m\tau$, that is,

$$\frac{d^2}{dx^2}\Psi_{\rm app}(x)\Big|_{m\tau}=\sum_n \Psi(n\tau)\frac{d^2}{dx^2}e^{-\alpha^2(x-n\tau)^2}\frac{\sin M(x-n\tau)}{\pi(x-n\tau)}\tau\Bigg|_{m\tau}$$

$$=\sum_n \Psi(n\tau)e^{-\alpha^2(x-n\tau)^2}\Bigg[2\alpha^2[-1+2\alpha^2(x-n\tau)^2]\frac{\sin M(x-n\tau)}{\pi(x-n\tau)}+\frac{-M^2\sin M(x-n\tau)}{\pi(x-n\tau)}$$

$$+\left\{\frac{-2M\cos M(x-n\tau)}{\pi(x-n\tau)^2}+\frac{2\sin M(x-n\tau)}{\pi(x-n\tau)^3}\right\}-4\alpha^2\left(\frac{M\cos M(x-n\tau)}{\pi}-\frac{\sin M(x-n\tau)}{\pi(x-n\tau)}\right)\Bigg]\tau\Bigg|_{m\tau}.$$

With our choice of grid spacing and M, $M\tau=\pi$, we can take advantage of Eq. (20). If $m\neq n$ only the cosine terms have a nonzero value. If $m=n$ all terms are nonzero. The sum of the terms in the curly brackets is obtained by employing the L'Hospital rule. By adding the different contributions one obtains the matrix elements given by Eqs. (21)–(22).

[1] V. Szalay, J. Chem. Phys. **108**, 2847 (1998).
[2] D. T. Colbert and W. H. Miller, J. Chem. Phys. **96**, 1982 (1992).
[3] J. R. Higgins, Bull. Am. Math. Soc. **12**, 45 (1985).
[4] H. Niquist, AIEE Trans. , 617 (1928).
[5] C. E. Shannon, Proc. IRE , 10 (1949).
[6] D. K. Hoffman, G. W. Wei, D. S. Zhang, and D. J. Kouri, Chem. Phys. Lett. **287**, 119 (1998).
[7] G. W. Wei, S. C. Althorpe, D. J. Kouri, and D. K. Hoffman, J. Chem. Phys. **108**, 7065 (1998).
[8] G. Charron and T. Carrington, Jr., Mol. Phys. **79**, 13 (1993).
[9] N. Hénon and C. Heiles, Astron. J. **69**, 73 (1964).
[10] B. Barbanis, Astron. J. **71**, 415 (1966).
[11] R. M. Stratt, N. C. Handy, and W. H. Miller, J. Chem. Phys. **71**, 3311 (1979).
[12] T. L. Marchioro II, M. Arnold, D. K. Hoffman, W. Zhu, Y. Huang, and D. J. Kouri, Phys. Rev. E **50**, 2320 (1994).
[13] G. Heinig and K. Rost, Linear Algebr. Appl. **275–276**, 225 (1998).
[14] K. S. Sorbie and N. C. Hancy, Mol. Phys. **33**, 1319 (1977).
[15] H. G. Yu and S. C. Smith, Ber. Bunsenges. Phys. Chem. **101**, 400 (1997).
[16] D. Neuhauser, J. Chem. Phys. **93**, 2611 (1990); M. D. Wall and D. Neuhauser, *ibid.* **102**, 8011 (1995); V. A. Mandelshtam and H. S. Taylor, *ibid.* **106**, 5085 (1997); D. J. Kouri, W. Zhu, G. Parker, and D. K. Hoffman, Chem. Phys. Lett. **238**, 3395 (1995); H. G. Yu and S. C. Smith, Ber. Bunsenges. Phys. Chem. **101**, 400 (1997).